UAV photogrammetry and deep learning-based grain size distribution analysis in a debris flow channel

*Samikshya Dahal [1], Fumitoshi Imaizumi [2], Tomoya Osada [2], Saleh Yousefi [3]

1. The United Graduate School of Agricultural Science, Gifu University
2. Faculty of Agriculture, Shizuoka University 3. AREEO, Iran

1. Introduction

Debris flow occurs as a fast-moving mixture of water and sediments triggered by intense rainfall or rapid snowmelt in mountainous regions. These flows travel through steep channel networks at high velocity and can transport large volumes of sediment, making them extremely powerful and destructive. As debris flows move downslope, they entrain, transport, and sort sediments of different sizes along the channel. Grain-size distribution patterns along the debris-flow channel provide important insights into initiation, transport, and deposition processes, making this parameter critical for debris-flow modelling and hazard assessment.

With advancements in computer vision, the machine learning model YOLOv8 has emerged as a state-of-the-art framework for object detection (Jocher et al., 2023). It has been successfully applied in fields as diverse as agriculture, medicine, security surveillance, and geohazard monitoring. Following its successful use in various disciplines, the YOLOv8 segmentation model also suggests strong applicability for identifying and delineating individual grains in images of debris-flow deposits. This capability can be directly applied to derive grain-size distributions for entire channels using an Unmanned Aerial Vehicle (UAV) photogrammetry. For this purpose, we trained and evaluated the YOLOv8 segmentation model's performance on UAV images of debris flow deposits and used it for grain size distribution analysis. This study aims to develop an automated, scalable, and repeatable approach for channel-scale grain size distribution mapping of debris flow deposits.

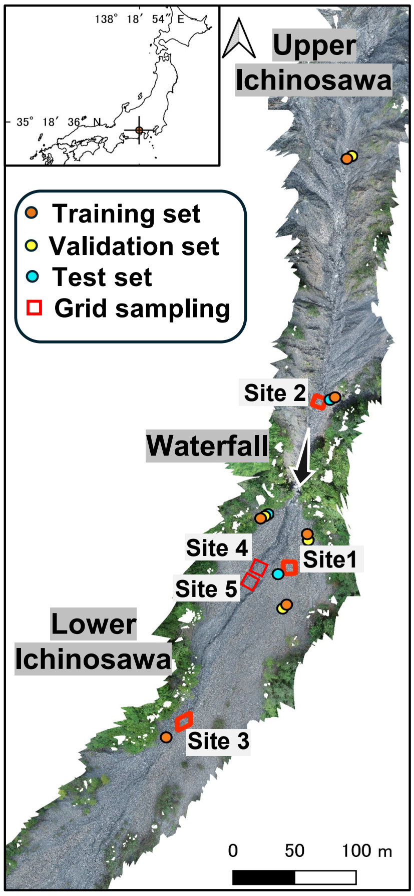

Figure 1. Map of Ichinosawa catchment in Ohya landslide (September 24, 2024)

2. Methodology

The study site is the debris flow channel deposit in the Ichinosawa catchment of the Ohya landslide, central Japan (Fig.1). The source of the channel bed sediments is Tertiary strata constituting well-jointed sandstone and highly fractured shale. UAV surveys of the debris flow channel were conducted on 24 September 2024 and 11 November 2024 from an altitude of 25m (8.8 mm px^{-1}) using a DJI Phantom 4 RTK. Separate orthomosaics were generated from each UAV survey using Structure-from-Motion photogrammetry, from which 2.5 × 2.5 m image patches were clipped at multiple locations across the channel deposits to prepare the training dataset. The dataset was prepared to train and compare two model variants: the multi-class model and the single-class model (Table 1). Four classes were defined for the multi-class model: bright (predominantly sandstone), dark (predominantly shale), vegetation (green vegetation nearby forest, and a few small plants), and wood. For the single-class model, bright and dark sediment labels were merged into a single grain class, and vegetation and wood were excluded as background.

Subsequent grain size distribution analysis was performed using the best-performing model. A threshold size was determined by comparing the manual label and YOLOv8 grain size distribution curves, below which grains were considered unreliably detected, and only grains exceeding this threshold were used for grain size distribution analysis. The YOLOv8-derived distributions were then constructed by sorting detected grains by minimum Feret diameter and expressing their cumulative contribution as a percentage of the total detected mask area. The grain size distribution was validated at five field sites using grid sampling techniques, where the b-axis of exposed coarse grains was measured using a measuring tape, and smaller grains were collected for sieve analysis.

Table 1. Dataset configuration

Parameter	Multi-class model	Single-class model
Training (70 %)	22 images / 5472 instances	22 images / 5342 instances
Validation (30%)	10 images / 2384 instances	10 images / 2313 instances
Test	6 images / 2126 instances	6 images / 2076 instances

3. Result and discussion

3.1. Performance of the multi-class and single-class YOLOv8 segmentation model

On comparing the segmentation performance of the multi-class and single-class models, the single-class model outperformed the multi-class model across all evaluation metrics (Table 2). The single-class model's average mask precision improved from 0.66 to 0.78, recall from 0.31 to 0.57, and mAP@0.5 from 0.40 to 0.68. In the confusion matrix, the multi-class model had bidirectional cross-class confusion between the two grain types; 9% of true bright grains were predicted as dark, and 10% of true dark grains were predicted as bright in the test set. Vegetation (mAP@0.5 of 0.21) and wood (mAP@0.5 of 0.45) had low accuracy, possibly because these classes are naturally scarce within the channel deposits and occur infrequently in training and testing images compared to sediment grains. Both models' recall value was lower due to difficulty in clearly separating small individual grains from the surrounding shadow and inter-grain matrix in UAV images, and especially for dark sediments. However, the single-class model eliminated cross-class confusion by treating all sediment grains as one category and wood and green vegetation as background.

Given the single-class model's superior performance over the multi-class model and reliable segmentation accuracy (mask mAP@0.5 = 0.68, precision = 0.78), the single-class model was selected for subsequent grain-size analysis. As the recall of 0.57 indicated potential under-detection of smaller grains, a minimum grain size threshold of 70 mm was determined by comparing the YOLOv8-derived grain size distribution curve with the manually measured one, for subsequent grain size analysis.

Table 2. Mask segmentation performance metrics

Model	Class	Precision	Recall	mAP@0.5
Multi-class	All (mean)	0.66	0.31	0.40
	Bright	0.77	0.50	0 .65
	Dark	0.42	0.28	0.30
	Wood	0.60	0.41	0.45
	Vegetation	0.84	0.07	0.21
Single-class	Sediment	0.78	0.57	0.68

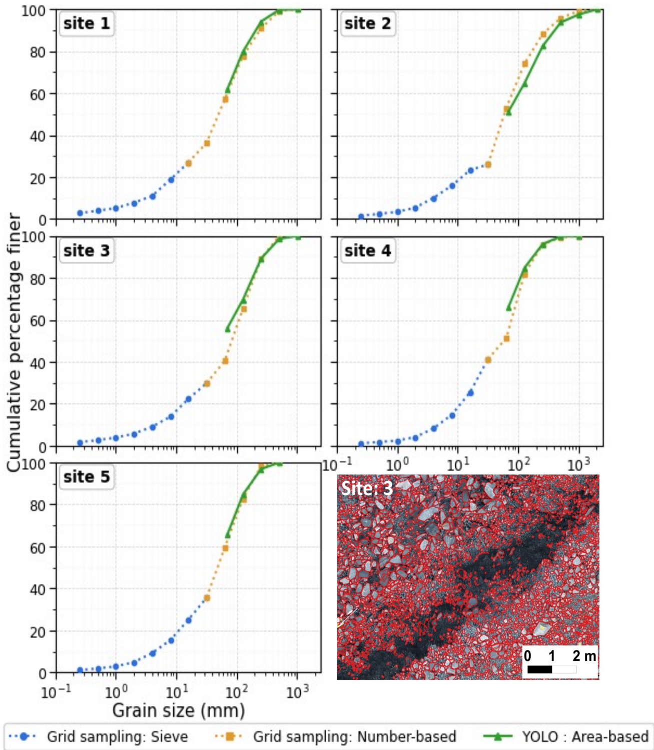

Figure 2. Validation of the YOLOv8's grain size distribution curve against field grid sampling at five sites

3.2. Grain size distribution analysis by YOLOv8

Grain size distribution curves obtained at four out of five sites shows strong agreement between YOLOv8 and grid sampling at D84 and D90, with Site 3 and Site 5 performing exceptionally well (errors within +4 to −13 mm, <10%), and Sites 1 and 4 showing acceptable differences of −14 to −28 mm (< 15%) (Fig. 2). The larger difference at Site 2 (+74 mm at D84, +112 mm at D90) is attributed to two factors: exposed fractured bedrock inadvertently segmented as individual grains, inflating the YOLOv8 distribution toward coarser sizes (Fig. 3); and comparatively large boulders occupying disproportionate pixel areas in YOLOv8's area-based detection relative to their single count in grid sampling. The former can be addressed by masking bedrock-exposed areas in UAV images before YOLOv8 inference; the latter, however, reflects a methodological difference between area-based and number-based sampling.

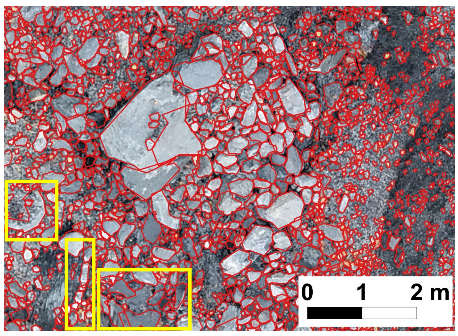

Figure 3. YOLOv8's segmentation at Site 2; yellow boxes highlight misidentified bedrock fractures and quartz veins segmented as individual grains

4. Conclusion

The single-class YOLOv8 model outperformed the multi-class model in segmentation metrics, and its automatic grain size distributions showed reliable agreement with field grid sampling, with D84 and D90 errors within 15% at four out of five sites, confirming its validity for coarse fraction characterization.

References

Jocher, G., Chaurasia, A. and Qiu, J. (2023): Ultralytics YOLOv8 (Version 8.0.0) [Software]. Available at: https://github.com/ultralytics/ultralytics